IEEE Photonics Journal
An IEEE Photonics Society Publication

Open Access

Energy-Efficient and Survivable Optical Access Network Based on Multilayer-Ring Structure

Volume 9, Number 4, August 2017

Yunxin Lv
Ning Jiang
Chenpeng Xue
Kun Qiu

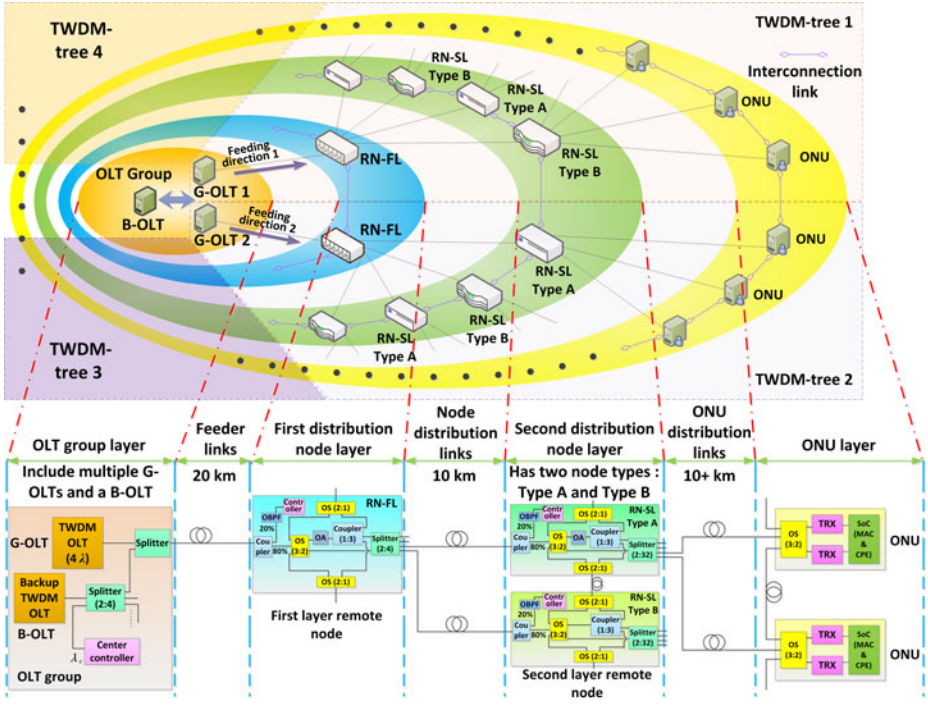

Structure of RAMOAN

DOI: 10.1109/JPHOT.2017.2726681
1943-0655 © 2017 IEEE

Energy-Efficient and Survivable Optical Access Network Based on Multilayer-Ring Structure

Yunxin Lv, Ning Jiang, Chenpeng Xue, and Kun Qiu

School of Communication and Information Engineering, University of Electronic Science and Technology of China, Chengdu 611731, China

DOI:10.1109/JPHOT.2017.2726681

Manuscript received May 18, 2017; revised June 21, 2017; accepted July 10, 2017. Date of publication July 13, 2017; date of current version July 26, 2017. This work was supported in part by the National Natural Science Foundation of China under Grants 61471087, 61301156, and 61671119, in part by the Specialized Research Fund for the Doctoral Program of Higher Education of China under Grant 20130185120007, and in part by the 111 project under Grant B14039. Corresponding author: N. Jiang (e-mail: uestc_nj@uestc.edu.cn).

Abstract: An energy-efficient and survivable optical access network structure is proposed and investigated. Based on a structure model of multilayer-ring, the access network is divided into four layers and modules on a same layer are interconnected as a ring. Therefore, multiple paths are available for optical network units to access an optical line terminal, which not only provides convenience in traffic aggregation, but also guarantees the survivability of network. With this structure, quantities of standby modules are reduced to decrease both capital cost and power cost. Large part of power can also be saved by turning OFF idle modules through traffic aggregation. Moreover, by controlling the optical switches deployed in remote node, elastic reach access is realized as well since amplification is optional on transmission links. Theoretical and numerical analyses indicate that the scheme shows great advantages on power saving, network survivability, as well as the system flexibility, and its energy efficiency performance can be further improved by operating in conjunction with energy-efficient resource scheduling scheme. It provides a potential structure for next generation optical access network.

Index Terms: Optical access network, energy efficiency, telecommunication network.

1. Introduction

The tremendous increment on the demand of broadband services leads to a rapid development of optical access network through the era. However, this development brings in a rigorous energy consumption problem as well. Due to the huge quantity of access networks, the access network segment has ranged among the top energy consumers in telecommunication networks [1]. Therefore, to benefit the further development of telecommunication networks, it is crucial to reduce the energy consumption of optical access network, and in the past decade, a vast amount of literature has been reported on the topic of energy-efficient optical access network.

In the most of the proposals so far, energy saving is achieved through studying three aspects: connecting structure, signal transmission, and multi-mode component based resource scheduling. In term of connecting structure, the studies focus on the proper utilization of the properties of optical communication to decrease the energy consumption of network. Benefiting from the nature of fiber,

the fiber-to-the-home (FTTH) access solution is proved as the most energy-efficient method for both user and operator [2]. By applying interconnection and aggregation among ONUs, power is saved via reducing active high-end components [3], [4]. These proposals take advantage of the low cost, high speed, and low loss properties of fiber network to reduce the power consumption of access network directly. In term of signal transmission, advanced multiplexing and signal processing techniques are studied and optimized to enhance the spectrum efficiency and energy efficiency. Based on orthogonal frequency division multiplexing (OFDM) technique, energy-efficient sampling scheme and transmission scheme are proposed [5], [6]. Recently, novel digital filter multiple access technique is reported as well to further reduce the cost on data delivery [7], [8]. These works improve the network efficiency by decreasing the cost on transmitting, receiving, and medium. As to the aspect of multi-mode component based resource scheduling, it is most widely studied. This is because due to the characteristic of access network, the network traffic pattern and user traffic pattern are severely varying, and there is enormous potential to save energy under low traffic load. Therefore, load-adaptively operating scheme is introduced to prevent energy wasting on idle or just partly used module by keeping the network capacity matching with actual user requirement [9], and numerous dynamic bandwidth allocation schemes are developed for ONU switching between active/sleeping statuses to further enhance energy efficiency [10]–[17].

These efforts greatly promote the energy efficiency of access network. However, it is not enough to meet the final goal. There is still a lot of works needing to be done to further decrease the energy consumption of future optical access network, such as how to solve the survivability problem while dealing with the energy efficiency issue since standby components greatly add the capital cost and power cost. ITU-T has provided some probable ways to implement network protection [18], and without doubt, providing a standby component for every module and link, namely fully protection, is the best solution to survivability issue. However, due to the additional cost, only compromised solution is adopted and part of the network is still vulnerable [19]. With the further development of optical access networks, future access network is facing the needs of large user capacity, long-reach access, high-speed access, flexible access, low-cost access and fully protected access. Since all these needs have penalties on power consumption of network and would influence energy efficiency, a proper solution which gives comprehensive consideration to energy efficiency, survivability, flexibility, large user capacity and wide-area coverage, is necessary to be explored for the future optical access network.

In this paper, a regional area metropolitan optical access network (RAMOAN) structure is proposed and investigated to meet the end. It is originated from time and wavelength division multiplexed passive optical network (TWDM-PON) but more energy-efficient, cost effective, and flexible while keeping the network fully protected. The network is hierarchically divided into four layers, and the modules on a same layer are interconnected together to form a ring. Therefore, a module can deliver data to two nearby modules in need. Consequently, multiple paths are available for an ONU to access an OLT, and many backup paths are provided. Thanks to these interconnection links, more traffic can be aggregated at low load, and more energy is saved correspondingly. To make things better, the cover radius of RAMOAN is elastic since amplifications become optional for transmission links in different scenarios. This paper is based on the work of [20]. However, there are many differences. The proposal in this paper can achieve automatic fault detection and automatic paths switching while the proposal in [20] cannot, and their detailed system structures and system performances are quite different. Moreover, this paper numerically evaluates the survivability, capital cost, and access reach flexibility issues while none of these works has been done in [20]. The rest of paper is organized as follow. Section 2 introduces the schematic structure and gives a thorough theoretical analysis of the proposed RAMOAN. Section 3 presents the numerical investigations on the performances of the scheme. Finally, a brief conclusion is summarized in Section 4.

2. Principles and Theoretical Analysis

In a typical TWDM-PON, ONUs are connected to the OLT via optical distribution network (ODN). Multiple passive remote nodes (RNs) are deployed in the ODN to aggregate fiber links from

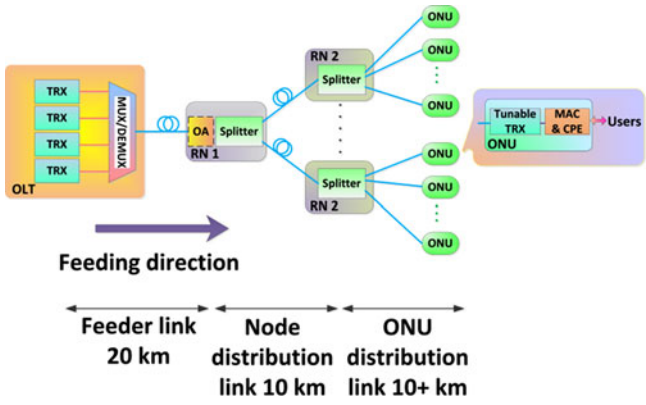

Fig. 1. Structure of a conventional TWDM-PON.

numerous ONUs. The structure of a TWDM-PON is shown in Fig. 1. For the purpose of reach extending, an optical amplifier (OA) can be deployed in the OLT-connected remote node. This architecture satisfies the requirements of large user capacity and long-reach access, but it is not protected. Therefore, there is a survivability problem in the conventional TWDM-PON, since that with the configuration of single feeder link and tree structure, any fault in modules or links would cause at least one ONU offline, and the breakdown of feeder link or higher level RN would be catastrophic. To deal with this issue and to provide fully protection to the network, conventional TWDM-PON would deploy standby modules and fibers and uses some 2:2 optical switches to control the employment of regular ones and standby ones, as that shown in [21]. However, it adds a lot of capital expenditure and introduces many idle components. Since usually multiple TWDM-PONs are required to be deployed to meet the accessing needs in a city area, if these networks build connections between same kind of modules in them, each module can perform as a standby one for other modules of the same kind. Therefore, the cost to perform protection could be greatly reduced. Moreover, the connections between different networks make it possible for wavelength-tunable ONU to access an OLT that belongs to another TWDM-PON. In this case, traffic can be highly aggregated to specified OLT under low load scenarios, and the number of active OLTs could be reduced. This could greatly enhance the energy saving effect since a sophisticated practical OLT consumes more power on its peripherals than on its transceivers. Therefore, inspired from these points, the energy-efficient, survivable, and flexible access structure of RAMOAN is proposed. In the following section, we discuss the RAMOAN thoroughly.

2.1 Structure and Operation Principles of RAMOAN

The schematic of RAMOAN is shown in Fig. 2. The whole network is constituted by four layers, which are the OLT group layer, the first distribution node layer (FDNL), the second distribution node layer (SDNL), and the ONU layer. The OLT group consists of multiple general four-wavelength TWDM OLTs (G-OLTs) and an additional backup OLT (B-OLT) with the same characteristics. In an OLT group, each G-OLT charges a feeder link of 20 km, and via optical splitters and fibers, the B-OLT is connected with all feeder links so that it can take over the work of any malfunctioning G-OLT. A transceiver embedded center controller is deployed at OLT group as well. By utilizing a specified wavelength, the center controller is able to communicate with the controllers resided at remote nodes to manage the operations of these nodes. The network subordinate to a G-OLT is similar to a TWDM-tree. For instantiation, four TWDM-trees are shown in Fig. 2.

Each feeder link is connected to a first layer remote node (RN-FL) on the FDNL. All RN-FLs are interconnected as a ring. A RN-FL is consisted of one 80:20 coupler, one optical bandpass filter (OBPF), one transceiver embedded controller, three optical switches (OSs, one 3:2 optical switch and two 2:1 optical switches), one optical amplifier, one 1:3 coupler, and one 2:4 splitter.

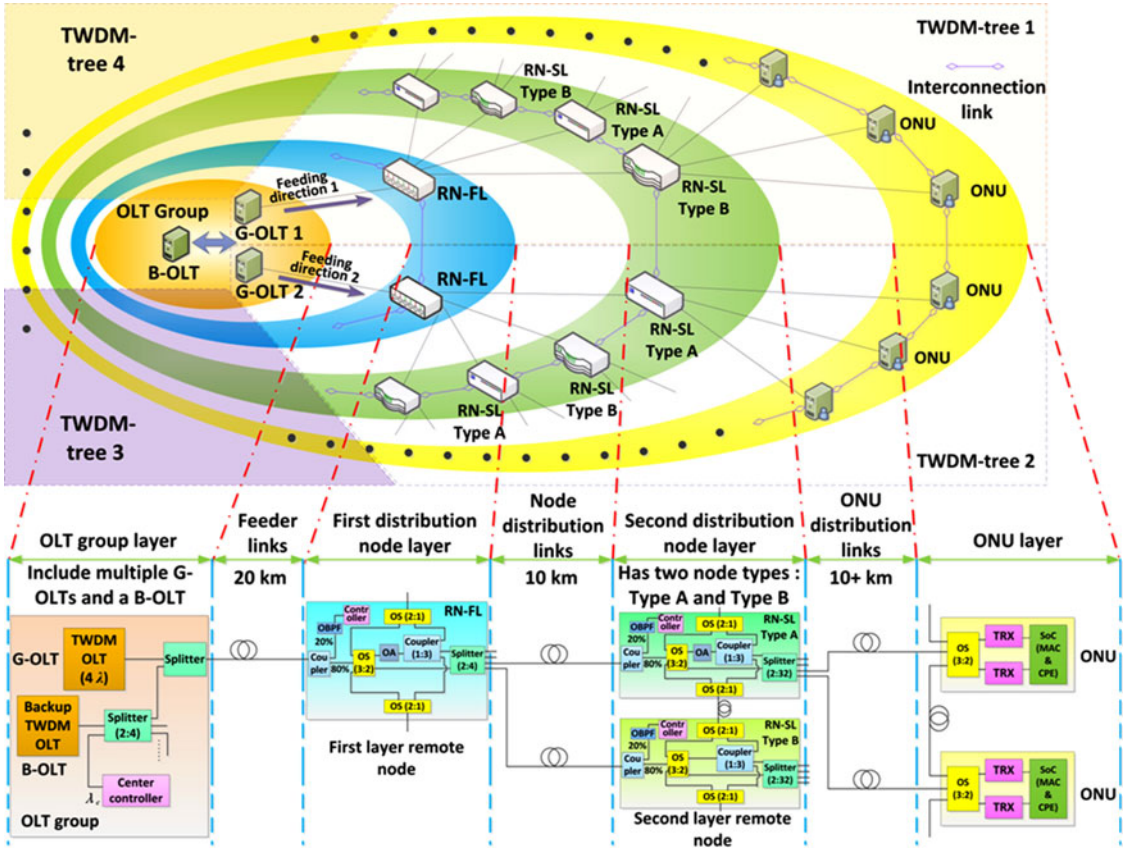

Fig. 2. Schematic of RAMOAN. (λ_c: wavelength for controlling messages.).

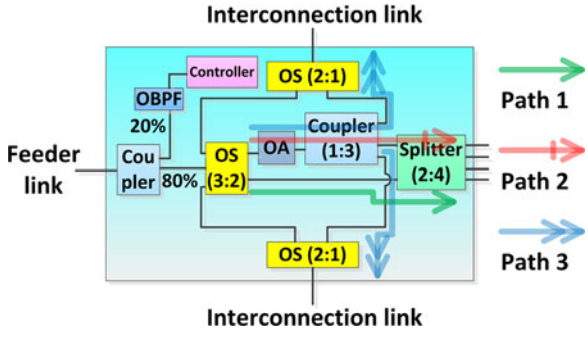

Fig. 3. Paths in RN-FL.

The function of the controller is to monitor the controlling signals from OLT side and to manage the operations of elements resided at the node, and it would send feedback to center controller as well once the statuses of these elements are changed. As shown in Fig. 3, by controlling the optical switches, three kinds of paths can be constructed in the RN-FL for the transmission of signals coming into the 3:2 optical switch. The first path is the direct distribution path, on which the 3:2 optical switch shifts its connection to the splitter and the optical amplifier is turned off. The second path is the amplification-distribution path, on which the connection of 3:2 optical switch is shifted to the optical amplifier to let signals traverse the optical amplifier, the coupler, and the splitter afterward. Therefore, this path could amplify signal, and network reach could be extended. The third path is the interconnection path, which is established based on shifting the connections

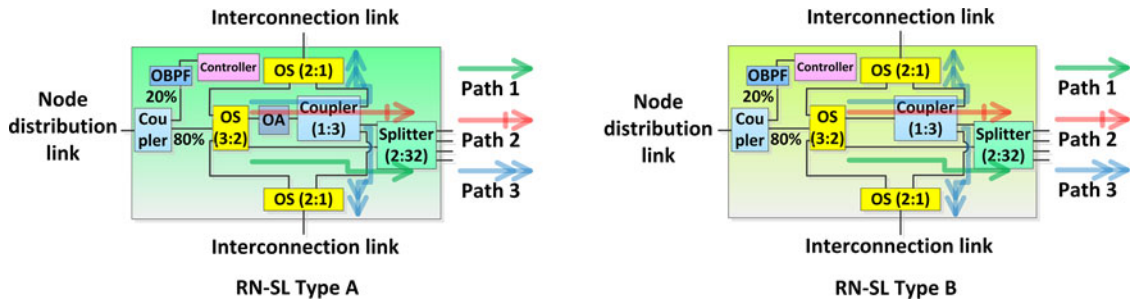

Fig. 4. Paths in two types of RN-SLs.

of 3:2 optical switch and 2:1 optical switch to the optical amplifier and the coupler, respectively. This path and the second path can be activated simultaneously, and on this path, signals would traverse the 3:2 optical switch, the optical amplifier, the coupler, and the 2:1 optical switch successively. Hence, via the third path, the RN-FL could deliver signals to two nearby RN-FLs on the same FDNL through the interconnection links between them. Correspondingly, a nearby RN-FL can utilize its 2:1 optical switch to directly forward the signals to its 3:2 optical switch, and establishes its own paths for transmission. Regard the RN-FL and its nearby RN-FLs as main-RN-FL and sub-RN-FLs. Consequently, when the traffic is low, the traffic from sub-RN-FLs can be aggregated by the main-RN-FL through the interconnection links, and the G-OLTs corresponding to these sub-RN-FLs can be turned off to save energy and resources. The interconnection link would also be used when a sub-RN-FL is having a fault in its feeder link. By indicating the corresponding ONUs to apply different wavelengths, the traffic of sub-RN-FL can be delivered to the main-RN-FL to finally reach the B-OLT through the links in the OLT group without interference.

The SDNL is similar to the FDNL. On the SDNL, all second layer remote nodes (RN-SLs) are interconnected together as a ring as well. Each RN-FL is connected with four RN-SLs on the SDNL through four 10 km node distribution links. In consideration of power budget and access reach, there are two types of RN-SLs derived, which are Type-A RN-SL and Type-B RN-SL. The Type-A RN-SL has a structure and function almost same as those of a RN-FL, but a 2:32 splitter is employed to replace the 2:4 splitter to increase the quantity of distribution ports. As to the Type-B RN-SL, it is similar to the Type-A RN-SL but removes the optical amplifier. Shown in Fig. 4, both types of RN-SLs can construct three kinds of paths to deliver the signals coming into their 3:2 optical switches as well. In all RN-SLs, the first direct distribution path is the major path. It is constructed by shifting the connection of 3:2 optical switch directly to the 2:32 splitter. The second amplification-distribution path in Type-A RN-SL is similar to that in a RN-FL, on which the 3:2 optical switch shifts its connection to the optical amplifier and signals would go through the 3:2 optical switch, the optical amplifier, the coupler, and the 2:32 splitter successively. Since optical amplifier is not deployed in the Type-B RN-SL, the second path there is renamed as coupled-distribution path, on which the 3:2 optical switch shifts its connection directly to the 1:3 coupler to let signals traverse the 2:32 splitter afterward. Same as that in a RN-FL, the third interconnection path in both types of RN-SL is established based on shifting the connections of 3:2 optical switch and 2:1 optical switch to the optical amplifier and the coupler, respectively, and it can be activated simultaneously with the second type of path. Therefore, through these 2:1 optical switches, the third path is connected with the interconnection links between RN-SLs. On the SDNL, the two types of RN-SLs are interconnected alternately, and the transmission mechanism between RN-SLs is basically same as that between RN-FLs. Hence, via the interconnection links on SDNL, a RN-SL can deliver signals to its nearby RN-SLs to perform traffic aggregation, and a node distribution link fault can be settled by delivering the traffic of the corresponding RN-SL to a nearby RN-SL. In addition, a RN-FL fault could be solved as well by indicating the corresponding RN-SLs to deliver traffic to the two RN-SLs belonging to two nearby RN-FLs.

On the ONU layer, each ONU is composed of a 3:2 optical switch, two tunable optical transceivers (TRXs), and a system on chip (SoC) which includes MAC and customer premise equipment (CPE). The structure of an ONU is shown in Fig. 5. There are three fiber links connecting to an ONU. Among

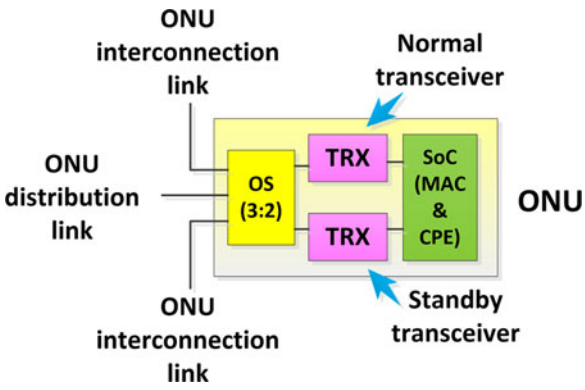

Fig. 5. Structure of an ONU.

them, one is ONU distribution link from RN-SL and spanning 10+ km, while the other two are ONU interconnection links that provide the ONU two links to connect with two nearby ONUs. Therefore, on the ONU layer, all ONUs can be interconnected as a ring. The two transceivers in an ONU are defined as normal transceiver and standby transceiver, respectively. The standby one would be activated not only under the condition that the normal one is malfunctioned, but also in the scenario that a nearby ONU requires to communicate with it through the ONU interconnection link. As a result, for each ONU, its data could be delivered to the OLT group via its nearby ONU by activating both transceivers of the nearby ONU. Hence, with two transceivers and ONU interconnection links, an ONU is protected in both conditions of transceiver malfunction and ONU distribution link fracture. In addition, the fault of a RN-SL can also be settled by connecting the corresponding ONUs in series through their ONU interconnection links to let these ONUs accessing another RN-SL via the ONU subordinate to the other RN-SL.

Overall, the four layers in RAMOAN build up three rings by interconnections. These connections make it possible for tunable ONUs to access all OLTs. Under low traffic, the RAMOAN could turn off some idle G-OLTs, and the corresponding ONUs would access other active G-OLTs via the interconnection links on FDNL and SDNL. Therefore, traffic aggregation and energy saving is achieved. Moreover, the multi-layer-ring structure builds up multiple backup paths for data transmission, and with fewer standby modules, the RAMOAN could be fully protected. This protection is reliable since the links are widely separated in physical location. To make things better, the controllers resided at OLT side and remote nodes make it possible for the RAMOAN to reconfigure its connections automatically in few milliseconds, and the controlling signals and ONU signals could jointly help RAMOAN to know the fault point when fault occurs. Additionally, the optional amplifications at remote nodes provide an elastic cover radius for the network, and the reach of the network could adapt to the demand of different scenarios to prevent energy wasting. The aggregated traffic also makes it more convenient for energy-efficient resource scheduling scheme to enhance its effect, and this will be investigated in the following part.

2.2 RAMOAN Cooperate With Resource Scheduling Scheme

In RAMOAN, the ONUs sharing a same wavelength are still using time division multiplexing (TDM) technique to access a same OLT transceiver. Therefore, those TDM-PON based energy-efficient resource scheduling schemes are still applicable to these ONUs. In this paper, for the ONUs accessing a same OLT transceiver, we adopt the load adaptive sequence arrangement (LASA) scheme that we proposed in [17] to save more energy in RAMOAN. In the following, we firstly introduce LASA in brief.

The LASA scheme is performed by dynamically setting a part of ONUs to be delayed polled in next cycle according to traffic load to rearrange the polling sequence of ONUs. The operation mechanism is as below. To avoid confusion, the mentioned OLTs in the following text of this paragraph are only

deployed with one transceiver. In each polling cycle, each ONU is assigned an individual label to confirm the polling sequence, and the label is added in gate/report message. Each ONU keeps the label obtained from gate message and then returns it back with bandwidth requirement by the report message. Assuming n ONUs are communicating with an OLT by TDM, and a factor θ is introduced to represent the number of ONUs that will be delayed polled in next cycle. Then according to the returned labels, the polling sequence for the current cycle, expressing by the returned labels, is refreshed as $\theta_0+1, \theta_0+2, \theta_0+3, \ldots, n, 1, 2, \ldots, \theta_0$, wherein θ_0 refers to the value of θ in the last cycle, and obeying the new polling sequence, the OLT is planning to send new labels $1, 2, \ldots, n$ to each ONU, respectively. In order to arrange the polling sequence effectively, here the OLT compares the current polling cycle time T_{cycle} with a threshold $T_{threshold} = T_{wakeup}/2 + T_{ONU}$, in which T_{ONU} and T_{wakeup} refer to the transmission time of an ONU in this cycle and the ONU wakeup transition time, respectively. If the cycle time is shorter than the threshold, as there is no chance to enlarge the idle time longer than the wakeup time, θ is set to zero. Then, the OLT calculates the idle time of each ONU by $T_{idle} = T_{cycle} - T_{ONU}$, and finally generates gate message containing the allocated bandwidth, idle time, and new label for each ONU. Otherwise, if the cycle time is longer than the threshold, the OLT calculates θ by

$$\theta = prox.\langle (T_{cycle} - T_{wakeup} + (n-1) \times T_{ONU})/(2 \times T_{ONU}) \rangle. \quad (1)$$

where n, T_{cycle}, T_{ONU}, and T_{wakeup} stand for the number of ONU sharing the OLT by TDM, the current polling cycle time, the transmission time of an ONU in this cycle, and the ONU wakeup transition time, respectively, and the operation $prox.\langle z \rangle$ denotes calculating the integer most proximal to z. In this case, the available idle time for the firstly polled θ ONUs in this cycle is set as $T_{idle\_l} = T_{cycle} + (n - \theta - 1) \times T_{ONU}$, while the other ONUs would obtain a relatively shorter idle time of $T_{idle\_s} = T_{cycle} - (\theta + 1) \times T_{ONU}$. According to these idle times, the OLT would calculate available sleeping time for each ONU, and then generates gate message containing allocated bandwidth, sleeping/idle time, and new label for each ONU. At ONU side, each ONU analyzes its transmission time, sleeping/idle time according to the received gate message, and executes exactly following the indications.

In the individual LASA scheme, when traffic is low and the cycle time is shorter than the threshold, it is still invalid on energy efficiency due to the too short polling cycle time. However, in RAMOAN, since all ONUs can be aggregated to communicate with a same OLT transceiver under low traffic load, the polling cycle time of the OLT transceiver could be extended, and too short cycle time can be prevented. Therefore, in the cooperative scheme, the RAMOAN firstly evaluates its total traffic load and decides the number of active OLT transceivers k. Then all ONUs are identically divided into k groups, and each group of ONUs would access an active OLT transceiver. After that, LASA is adopted among ONUs sharing a same OLT transceiver. In this way, more ONUs would access a same OLT transceiver, and the energy-inefficiency of LASA scheme under low traffic load can be avoided. Consequently, enhanced energy saving performance can be achieved for RAMOAN, which is numerically investigated in next chapter.

3. Numerical Investigations and Results

In the simulations for results evaluation, four four-wavelength 40G G-OLTs are deployed in the OLT group and 512 wavelength-tunable ONUs are served in RAMOAN. Each ONU is provided a bandwidth of 312.5 Mbits. Four feeder links are evenly distributed around and the angle between two adjacent feeder links is 90 degree. The distribution links from a remote node are evenly distributed as well. Since a conventional four-wavelength 40G TWDM network could only afford 128 ONUs with a same per-ONU bandwidth of 312.5 Mbits, in order to compare performances under the conditions of identical network scale and user capacity, four same conventional TWDM networks constitute a network system to represent the performance of conventional TWDM scheme. In this network system, the OLTs of the TWDM networks are centralized at a same point, and optical amplifiers are equipped in these TWDM networks. The layouts of RAMOAN and the TWDM network system are displayed in Fig. 6(a) and (b), respectively.

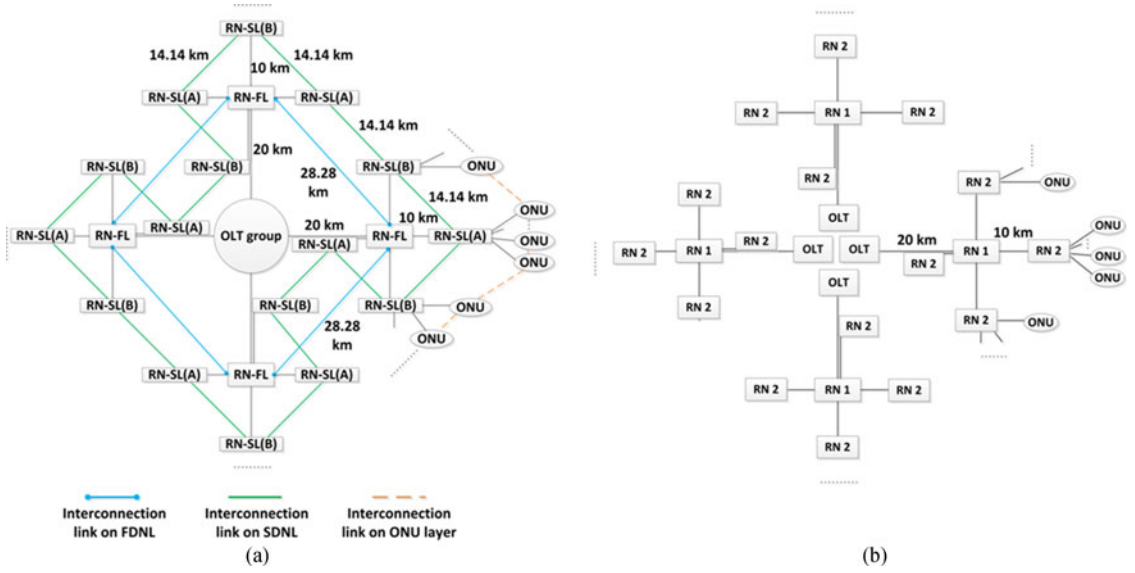

Fig. 6. (a) Layout of RAMOAN; (b) layout of the TWDM network system.

TABLE 1
Availabilities of Network Elements

Element	Availability	Element	Availability
OLT transceiver	0.9999900	OA	0.9999960
OLT subsystem	0.9999957	OS (3:2)	0.9999920
Booster	0.9999960	OS (2:1)	0.9999920
MUX/DEMUX	0.9999993	Coupler (1:3)	0.9999993
OS (2:2)	0.9999920	Splitter (2:4)	0.9999991
Card space	–	Splitter (2:32)	0.9999980
Splitter (2:1)	0.9999993	ONU transceiver	0.9999840
Splitter (1:4)	0.9999992	ONU subsystem	0.9999806
80:20 Coupler	0.9999993	Fiber	0.9999429/km
Splitter (1:32)	0.9999987		

3.1 Features of RAMOAN

The survivability issue is given the top priority since it is of great significance to operators. According to the reports in [22], the availabilities of network elements are organized and listed in Table 1. In the simulations, three network schemes are evaluated, which are conventional TWDM scheme, conventional TWDM scheme that is fully protected, and RAMOAN. In the fully protected conventional TWDM scheme, each of the four conventional TWDM networks is protected by deploying a standby module/link for each module and link in it, and some 2:2 optical switches are deployed to control the employment of regular ones and standby ones [21]. Transceiver (operating on a specified wavelength) embedded controllers are deployed at OLT and remote nodes to monitor the availability of transmission links and manage the operations of these optical switches. By analyzing the losses of controlling signals and user signals, this network system could find the fault point and settle the issue automatically when fault occurs. The schematic structure of a fully protected TWDM network

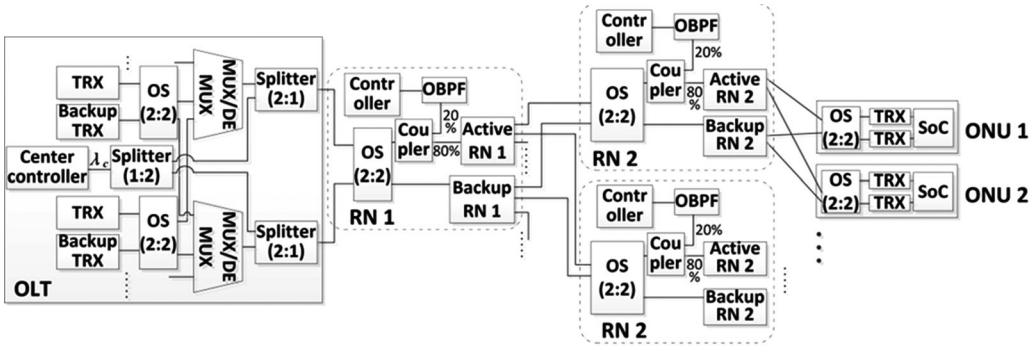

Fig. 7. Structure of a conventional fully protected TWDM network.

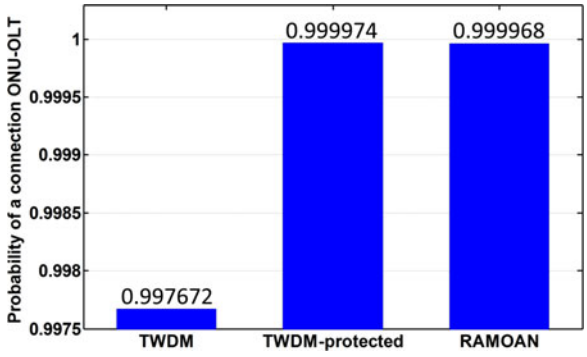

Fig. 8. Probability of an intact connection from an ONU to OLT.

is shown in Fig. 7. For practical purpose, if a module or link in RAMOAN is malfunctioning, we only consider the two nearest modules or links as its alternates. Fig. 8 depicts the probability of an intact connection between an ONU and OLT in the three schemes. Here, the length of ONU distribution link is set as 10 km. Detailed calculation method is given in Appendix 1. It is indicated that in the conventional TWDM scheme, an arbitrary ONU is facing an ONU-OLT connection failing rate of 0.2328% (availability level: two '9s'), while the figure for fully protected TWDM scheme is only of 0.0026% (availability level: four '9s'). The RAMOAN also shows a low failing rate on building an intact ONU-OLT connection for an arbitrary ONU, and an ONU in the RAMOAN would face an ONU-OLT connection failing rate of 0.0032% (availability level: four '9s'). This result intuitively shows that the unprotected TWDM scheme is facing a great survivability issue since there are numerous ONU-OLT connections in the network, and this scheme is not suitable for practical employment for the reason that ONU losing is never acceptable. By contrast, the fully protected TWDM scheme and RAMOAN are survivable since they can provide a same high level of availability for their ONU-OLT connections. This emphasizes the essentiality of performing protection during network operation.

With such a prominent survivability enhancement, whether the RAMOAN induces a high capital cost due to its complex structure is another crucial point that needs to be evaluated. According to the reports in [21], [23], and [24], the capital costs of different network elements are organized and listed by Table 2. Then the total capital cost of each network scheme can be calculated by adding up the costs for its elements. Here, it should be mentioned that the cost for trenching is not discussed in this paper since this uncertain cost will widely vary under different cases due to workforce price changing or trench sharing. Shown in Fig. 9, since the components for survivability enhancement bring in an additional capital cost, the fully protected TWDM scheme and the RAMOAN are with higher capital cost. However, the RAMOAN only adds about 37% of cost in relative to the unprotected TWDM scheme, and its cost is about 63% lesser than that of the fully protected TWDM scheme. This is because in RAMOAN, much fewer elements are deployed for standby.

TABLE 2
Costs of Network Elements

Element	Cost (dollar)	Element	Cost (dollar)
OLT transceiver	1500	Splitter (1:32)	400
OLT MAC	600	OA	2000
Shelf port card	660	OS (3:2)	90
L2 switch	200	OS (2:1)	70
Booster	1500	Coupler (1:3)	40
MUX/DEMUX	150	Splitter (2:4)	100
OS (2:2)	80	Splitter (2:32)	420
Card space	5000	ONU transceiver	175
Splitter (2:1)	40	ONU MAC	100
Splitter (1:4)	70	OBPF	120
80:20 Coupler	40	Fiber	150/km
Controller	80		

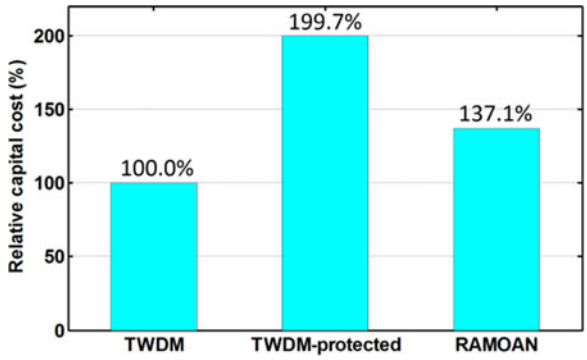

Fig. 9. Capital cost evaluation.

According to the former results, it can be concluded that the RAMOAN perfectly ensures the survivability of transmissions between ONUs and OLT, and greatly decreases the capital expenditure in comparison with the conventional network scheme that has a same level of survivability. This means the RAMOAN has prominent practical value. Therefore, performances of RAMOAN are further evaluated to deeply exam its suitability for future access network.

To provide accesses for users in a wide area, future access network needs to have 40+km cover radius. Therefore, the network cover radius of RAMOAN is then measured to confirm its fitness for metropolitan-access. The power costs and insertion losses (ILs) of elements are obtained from [21] and [23]–[26], and they are categorized and listed in the Table 3. The insertion loss of fiber, the launch power of transmitter, and the sensitivity of receiver are 0.25 dB/km, 6 dBm, and −30 dBm, respectively [21], [23].

Note that center controller needs to exchange information with the controllers resided in RN-FLs and RN-SLs to manage the connections of network. When the RAMOAN tries to send control messages to reconfigure the connections, the center controller would firstly send command messages to RN-FLs to activate their second amplifier paths, and then send control messages to RN-SLs. After receiving the confirmation signals from RN-SLs, the center controller would send control messages to RN-FLs. In this way, the information exchange between controllers and center controller

TABLE 3
Power Costs and Insertion Losses of Network Elements

	Per OLT (4λ)	Distribution network	Per ONU
TWDM	OLT MAC: 4 W Per OLT 10 G TRX: 3.5 W Shelf port card: 26 W Booster: 24 W Gain = 4 dB L2 switch: 27 W MUX/DEMUX: IL = 1.5 dB Controller: 1.5 W Splitter (2:1): IL = 3.8 dB OS (2:2): 0.2 W, IL = 0.5 dB Card space: 2 × 60 W Splitter (1:2): IL = 3.8 dB	OS (2:2): 0.2 W, IL = 0.5 dB Splitter (1:4): IL = 7 dB Splitter (1:32): IL = 16.6 dB OA: 50 W, Gain = 20 dB Controller: 1.5 W 80:20 coupler: IL = 1 dB 20:80 coupler: IL = 7 dB OBPF: IL = 1.5 dB	OS (2:2): 0.2 W, IL = 0.5 dB Per TRX: 3.5 W SoC (MAC & CPE): 2 W
RAMOAN	OLT MAC: 4 W Per OLT 10 G TRX: 3.5 W Shelf port card: 26 W Booster: 24 W Gain = 4 dB L2 switch: 27 W MUX/DEMUX: IL = 1.5 dB Controller: 1.5 W Splitter (2:1): IL = 3.8 dB Splitter (2:4): IL = 7.4 dB Card space: 60 W	OS (3:2): 0.2 W, IL = 0.5 dB OS (2:1): 0.2 W, IL = 0.5 dB OA: 50 W, Gain = 20 dB Coupler (1:3): IL = 5.5 dB Splitter (2:4): IL = 7.4 dB Splitter (2:32): IL = 17.5 dB Controller: 1.5 W 80:20 coupler: IL = 1 dB 20:80 coupler: IL = 7 dB OBPF: IL = 1.5 dB	OS (3:2): 0.2 W, IL=0.5 dB Per TRX: 3.5 W SoC (MAC & CPE): 2 W

could be ensured, and with the controlling signal launch power of 6 dBm and receiver sensitivity of −30 dBm, the received power of controlling signal would be −18.7 dBm and −15.6 dBm at RN-FL and RN-SL, respectively.

Fig. 10 firstly shows the active links and modules in RAMOAN under different load conditions. When the traffic is below 0.25, three G-OLTs are turned off. The three RN-FLs corresponding to these G-OLTs are regarded as sub-RN-FLs, and their traffic is aggregated at the other RN-FL called as main-RN-FL to deliver to the only active G-OLT. In this case, two sub-RN-FLs (marked in green) would employ the direct distribution path and turn off their amplifiers, because the reach is able to meet the beyond-40 km requirement. When the traffic load is ranged from 0.25 to 0.50, two G-OLTs are turned off, and the other two active G-OLTs that feed the RN-FLs in two opposite directions manage the operation of network. Specially, in the load range from 0.50 to 2/3, one G-OLT and its feeding RN-FL are turned off. In this condition, the RN-SLs subordinate to the inactive RN-FL are divided into two groups, and each group would access a nearby RN-SL that is subordinate to another RN-FL to maintain transmission. When the traffic is above 2/3, all G-OLTs are turned on to serve the ONUs, and the network is operating as four individual TWDM networks.

The minimal cover radius of RAMOAN versus normalized traffic load is shown in Fig. 11(a). Here, for practical purpose, the ONU-OLT transmission link that affords the shortest reach in RAMOAN is used to measure the minimal cover radius of RAMOAN. Since some interconnection links may be traversed, the access reach of an ONU-OLT transmission link in RAMOAN is calculated by adding the length of feeder link, the length of node distribution link, and the available reach of final distribution link up. In the scenario that the traffic load is below 0.50, the ONU-OLT transmission link passing through the sub-RN-FL that its amplifier is turned off and locates just beside main-RN-FL, determines the minimal cover radius of RAMOAN. Under this circumstance, the cover radius of the network is small and just exceeds the 40 km radius requirement by about 9 km. When the traffic load is from 0.50 to 2/3, the minimal cover radius is evaluated according to the available reach of the ONU-OLT transmission link distributed by the type-B RN-SL, where the type-B RN-SL refers to the one that is subordinate to the active RN-FL and is interconnected with the type-A RN-SL

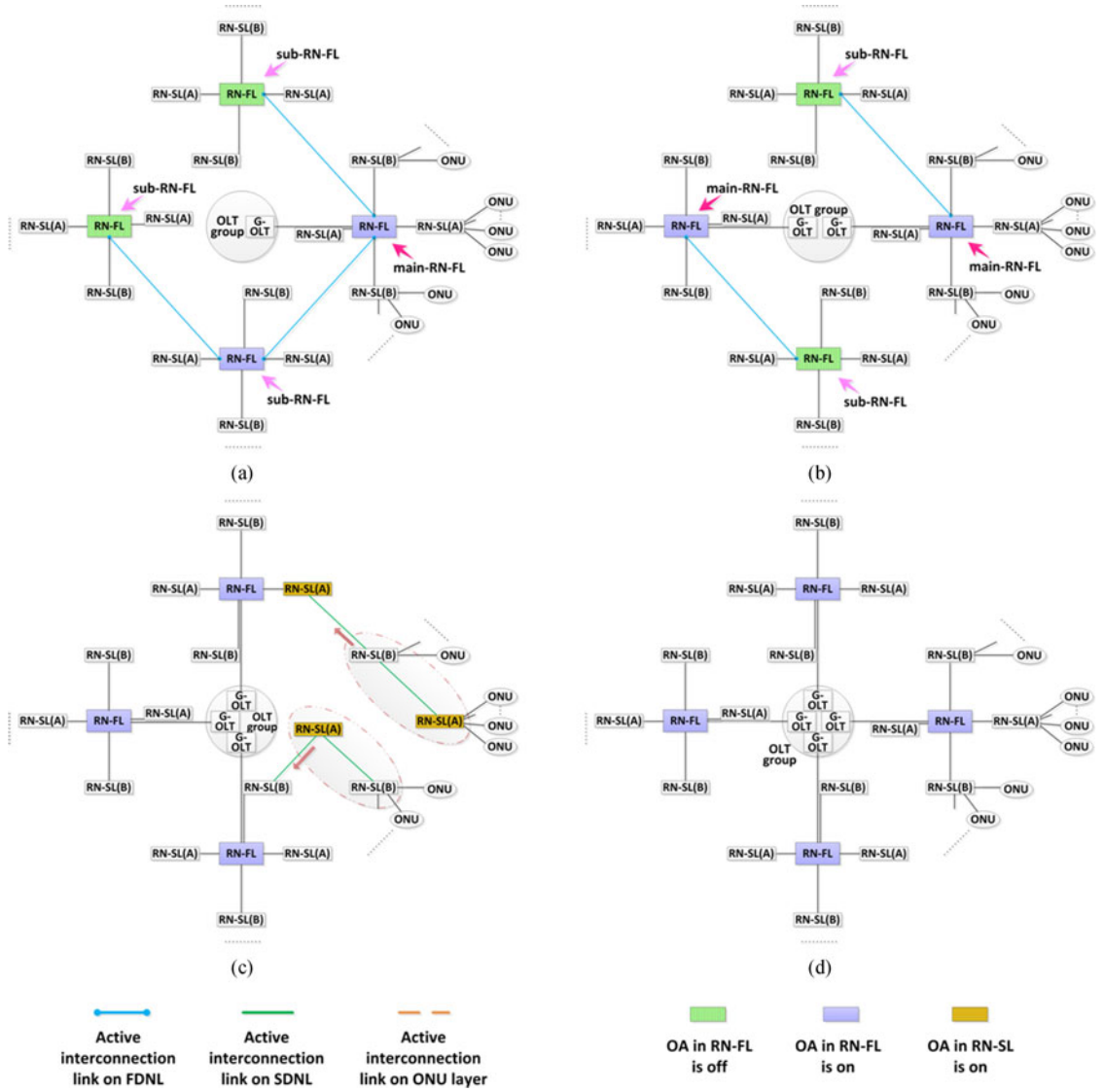

Fig. 10. Active links and modules in RAMOAN under different traffic load conditions: (a) normalized traffic load is between 0 and 0.25; (b) normalized traffic load is between 0.25 and 0.50; (c) normalized traffic load is between 0.50 and 2/3; (d) normalized traffic load is between 2/3 and 1.

belonging to the inactive RN-FL. In this case, the minimal cover radius of the network is about 61 km. When the traffic load is above 2/3, the reach of the ONU-OLT transmission link down through a single TWDM-tree equals the minimal cover radius, and it exceeds 83 km since interconnection links are not traversed. The minimal cover radiuses of the two TWDM schemes are also shown in Fig. 11(a) for comparison. Here, although the unprotected TWDM scheme is not suitable for practical use due to its high ONU losing rate, it is evaluated in our simulation as well since it can show the penalties of performing protection. With the deployment of amplifiers, the cover radiuses of the two TWDM schemes are relatively larger than that of RAMOAN, and the unprotected TWDM scheme outperforms the fully protected one since it does not suffer the insertion loss induced by component switching devices. Detailed calculation method for minimal access reach can be found in Appendix 2.

It should be noted that the aforementioned minimal cover radius of RAMOAN is calculated under normal operation condition. However, under the emergency conditions such as G-OLT failure, an

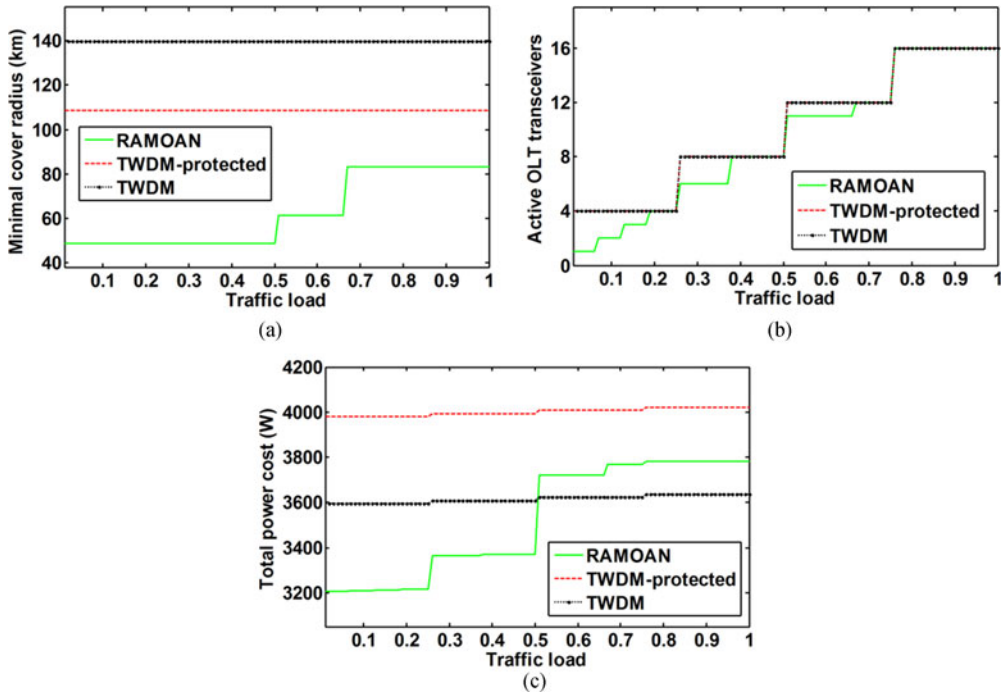

Fig. 11. Performances comparison between RAMOAN and two TWDM schemes: (a) minimal cover radius; (b) usage of transceivers; (c) total network power consumption.

additional 2:4 splitter should be traversed to access the B-OLT. Therefore, an additional 7.4 dB of insertion loss is emerged and the available reach would be reduced. Hence, under emergency cases, RAMOAN would activate interconnection links as few as possible to ensure the reach of ONU-OLT transmission links. Then in the case of G-OLT failure, since the RN-FL corresponding to the faulted G-OLT can turn on its amplifier to employ the amplification-distribution path, the minimal access reach is

$$\begin{aligned} Reach = (&Power_{launch} + Gain_{booster} - IL_{MUX} - IL_{splitter_{2:4}} - IL_{splitter_{2:1}} - IL_{80:20coupler} - IL_{RN-FL_{path\_2}} \\ &+ Gain_{OA} - IL_{80:20coupler} - IL_{RN-SL_{path\_1}} - IL_{OS_{3:2}} - Sensitivity_{receiver})/IL_{fiber} \\ &= 53.6\,\text{km}, \end{aligned} \tag{2}$$

which meets the 40 km requirement as well. This 7.4 dB insertion loss should also be counted under the scenario of feeder link fracture. Nevertheless, since two RN-FLs are traversed and signal can be amplified twice, the available reach would be longer than 53.6 km because the insertion loss of interconnection link is smaller than the gain from amplifier. Therefore, a fully protected 40 km cover radius is easily ensured in the RAMOAN.

In Fig. 11(b), the usage of transceivers at OLT side is shown. Under the low traffic scenarios, the RAMOAN and the two TWDM schemes turn off some transceivers. It is easy to understand that the two TWDM schemes show a same performance since standby components are not activated. However, the RAMOAN obviously occupies fewer transceivers under low traffic scenarios due to its traffic aggregation advantage. Therefore, fewer wavelengths would be used in RAMOAN, and the wavelength efficiency is improved.

Finally, by adding up the power costs of active network elements, the total network power costs of RAMOAN and two TWDM schemes can be calculated and the result is shown in Fig. 11(c). Here, it should be mentioned that in RAMOAN and fully protected TWDM scheme, all the controllers at both OLT side and remote nodes are always activated. It is clear that the power costs of three schemes rise with the growth of traffic load. In RAMOAN, the total power cost of the network is low when the

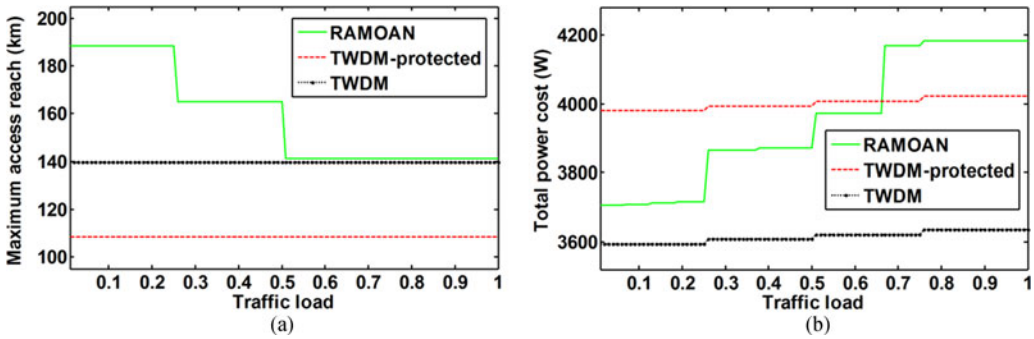

Fig. 12. Performances comparison: (a) maximal access reach; (b) total power cost.

traffic is below 0.25. This is because three G-OLTs are turned off and a large amount of power is saved, and additional power can be saved by turning off more OLT transceivers under a lower load. When the traffic is in the range of 0.25 to 0.5, two G-OLTs are turned off, and the total network power cost is increased for the increment of active G-OLTs and OLT transceivers. The power cost of RAMOAN is severely raised in the load range from 0.51 to 2/3. This phenomenon is resulted by the additional activated G-OLT and the activation of three optical amplifiers in RN-SLs. In the scenario that traffic load is above 2/3, all four G-OLTs are activated and the total network power cost is further increased. It reaches the maximum value when the traffic load exceeds 0.75, since all OLT transceivers are needed to be turned on to serve ONUs. As to the two TWDM schemes, although they can turn off some transceivers, only a small part of power is saved under low traffic scenarios. This is because the power cost of a transceiver is too small when comparing with that of an entire OLT. Moreover, since controller, switching devices, and extra space for standby modules bring additional power cost to the fully protected TWDM scheme, its power cost is very high under all load conditions. It is obvious that by turning off some G-OLTs and aggregating traffic to other active G-OLTs, the RAMOAN greatly reduces the power cost of network under low traffic load, and the power saving effect can be enhanced through further turning off some transceivers. Thus, although the power cost on controllers, optical amplifiers, and switches increases, the power efficiency performance of RAMOAN is outstanding, especially under low traffic load. According to the evaluation, the power saving ratio of RAMOAN can be up to 19.5% and 10.8% in relative to the fully protected TWDM scheme and the unprotected TWDM scheme, respectively. It should be noticed that under high load conditions, the unprotected TWDM scheme costs less power than the RAMOAN. However, this network is not protected and has a survivability issue. Since the fully protected TWDM scheme still costs at least 240 W of power more than the RAMOAN under high traffic load, it can be concluded that the RAMOAN possesses the power efficiency advantage.

The results shown by Fig. 11 indicate that the two TWDM schemes have advantages on minimal cover radius. However, amplification is not optional on their transmission links during operation, and their access reaches are not flexible. This may result in the waste of resources under various practical conditions. In contrast, the RAMOAN shows great flexibility on its access reach, and this balance between access reach and active amplifiers could make the network more efficient, which further improves the practical value of the scheme. Although under short reach access requirement, the minimal cover radiuses of these two TWDM schemes could be reduced by 80 km and a power cost of 200 W could be saved by removing the amplifiers, the minimal cover radius of fully protected TWDM scheme would only be 28.4 km, and the RAMOAN would still be more energy-efficient in comparison with the two TWDM schemes under low traffic load according to Fig. 11(c). Moreover, in this scenario, the RAMOAN still keeps its power efficiency advantage with respect to the fully protected TWDM scheme under high load conditions.

In correspondence to the minimal cover radius depicted in Fig. 11(a), Fig. 12(a) shows the maximal access reach of RAMOAN as a further evaluation of the access reach flexibility. With the

TABLE 4
Network and Protocol Parameters

Parameter	Value
Line rate (single wavelength)	10 Gbit/s
Maximum cycle time	10 ms
Normalized traffic load	0.01–1
Inter frame gap	1 μs
ONU wakeup transition time	2 ms
Average packet size	791 bytes
Length of ONU distribution link	10 km

connecting structures same as those shown in Fig. 10, the maximal access reach is measured according to the maximal available reach of an ONU-OLT transmission link in RAMOAN under the condition that all available amplifiers are activated. It is evident that the RAMOAN can provide a longer access reach than the two TWDM schemes. With the growth of traffic load, the maximum access reach of RAMOAN decreases. This is because under low load, an ONU-OLT transmission link would traverse more remote nodes, and more optical amplifiers can be employed. Fig. 12(b) provides the corresponding network power cost. Here, since all available optical amplifiers are turned on, the total power cost of RAMOAN is relatively higher than that of the unprotected TWDM scheme. Nevertheless, it is still more efficient than the fully protected TWDM scheme when traffic load is below 2/3. Comparing the results shown in Figs. 11 and 12, the access reach flexibility of RAMOAN is clearly observed. However, a part of energy saving effect is offset by achieving the long reach access.

In all, although the conventional unprotected TWDM scheme shows some advantages on capital cost and operational cost, the crucial survivability problem could lead the scheme not suitable for practical deployment and make it necessary to adopt protection. However, the protection related components would bring in some penalties and totally counteract these advantages. By contrast, the RAMOAN could perfectly balance the ends. Comparing to the unprotected TWDM scheme, it strongly ensures the survivability of ONU-OLT connections and introduces lesser penalty on power cost and capital cost with respect to the conventional fully protected TWDM scheme. Moreover, the proposed RAMOAN has flexible access reach, and it outperforms the two TWDM schemes on energy efficiency under low load conditions. These advantages ensure the practicability of RAMOAN and make it very suitable for future access network.

3.2 Cooperation of RAMOAN and LASA

To thoroughly investigate the RAMOAN structure, the cooperation of the RAMOAN and the energy-efficient resource scheduling scheme LASA (RAMOAN-LASA) is further evaluated with 512 ONUs. Since LASA is a TDM based scheme, it is performed on ONUs sharing a same OLT transceiver. Table. 4 lists the relevant network parameters. For simplicity, network load is evenly distributed to every ONU.

Fig. 13(a) shows the energy consumption of RAMOAN when LASA is adopted. The energy costs of the two TWDM schemes are also shown for comparison. It can be observed that the energy costs of the two TWDM schemes increase with traffic load since more OLT transceivers are turned on. By contrast, the figure for RAMOAN-LASA is quite different. With the growth of traffic load, it shows that the energy cost of RAMOAN-LASA fluctuates severely and drops nine times. This phenomenon is resulted by the following reasons. When traffic load is growing from 0.01 to 1,

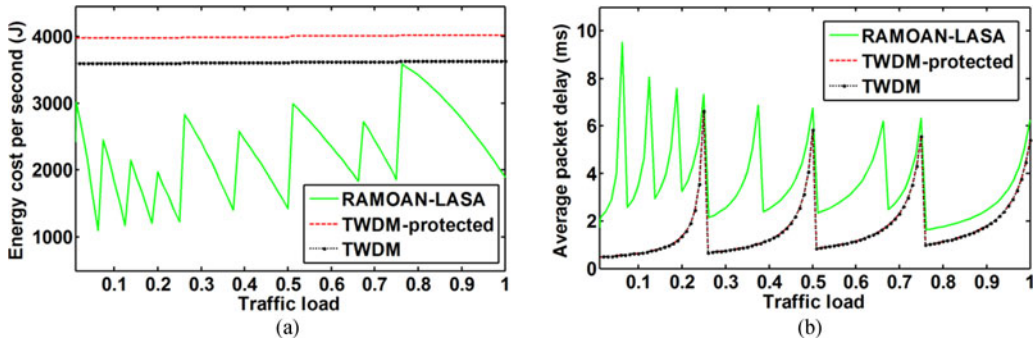

Fig. 13. Performances comparison: (a) energy consumption of network; (b) average packet delay.

nine different numbers of active OLT transceivers are observed [see Fig. 11(b)]. Corresponding to each case, there is specified number of ONUs communicating with an OLT transceiver. Commonly, $\{512/k\}$ ONUs are set to be served by an OLT transceiver, where k refers to the number of active OLT transceivers, and the operation $\{x\}$ represents calculating the integer that is the smallest but larger than x. In the particular case that 11 OLT transceivers are turned on (traffic load is from 0.50 to 2/3), each OLT transceiver is set to serve 48 ONUs due to the restriction of physical links. Here, the OLT transceivers that are actually serving fewer ONUs would extend their TDM polling cycle time by staying at idle mode to keep a same cycle length as other active OLT transceivers for the convenience of operation. Similarly, the cycle time difference induced by different propagation delays would be compensated by giving additional idle times to the OLT transceivers that have shorter polling cycle times. Consider an OLT transceiver that is serving a given number of ONUs. When the traffic gets heavier, the cycle time increases, and ONUs could sleep for a longer time in each cycle. Consequently, the energy cost of ONUs decreases, and the energy cost of network drops down. When the traffic is too heavy and the OLT transceiver cannot afford so many ONUs, additional OLT transceiver is turned on to share the traffic. Then, each OLT transceiver serves fewer ONUs and the cycle time becomes short again. Correspondingly, the available sleeping time of ONUs decreases, and this finally leads to the stepping up of network energy cost. In general, nine drops and eight abrupt rises are observed in the figure for the cooperative scheme. It can be found that in comparison with the two TWDM schemes, the RAMOAN saves much more energy by cooperating with LASA, and substantial energy saving could also be achieved under high load conditions.

Fig. 13(b) shows the average packet delay of the cooperative scheme. Corresponding to the nine drops in Fig. 13(a), the average packet delay of RAMOAN-LASA scheme rises nine times. This is because in the context that an OLT transceiver is serving a given number of ONUs, packet delay increases with the growth of traffic since more data is piled up for transmission. However, when the traffic grows too heavy and additional OLT transceivers are activated, fewer ONUs are served by a same OLT transceiver. Therefore, the traffic of an OLT transceiver suddenly goes down, and the packet delay is severely decreased. Finally, nine rises and eight sudden drops are occurred. It is indicated that the packet delay fluctuates between 2 ms and 10 ms, which means that the system is able to support delay sensitive services according to [27]. For comparison, the packet delays of the two TWDM schemes are shown as well. These two curves overlap each other since the two schemes can be considered same under normal operating condition. Similar to that in RAMOAN-LASA, four rises and three sudden drops are observed in either of the two TWDM schemes due to the growth of traffic load and the variation on the number of active OLT transceivers. It is shown that the average packet delays of the two TWDM schemes are relatively lower than that of RAMOAN-LASA, because their polling cycle lengths are shorter and polling sequences are not changed.

Overall, by adopting the LASA scheme, the proposed RAMOAN shows prominent energy saving property, and it is able to provide a satisfactory service quality.

4. Conclusion

In this paper, a future optical access network structure called RAMOAN is proposed and thoroughly investigated. By the four-layer-three-ring structure, it provides wide area access with advantages on power efficiency, survivability, as well as flexibility. With the help of optical switches and interconnection links, ONU-OLT transmission paths are very flexible, and with only a few standby components, the network survivability is ensured. The flexibility of ONU-OLT transmission paths also makes it more convenient to aggregate traffic and resources, and more power is saved. Moreover, flexible access reach is realized since amplification at remote node is optional for ONU-OLT transmission links. The simulation results demonstrated that the RAMOAN could save large part of power while providing fully protected ONU-OLT transmission links, and it is cost effective with respect to the conventional fully protected TWDM network. In addition, the cooperation of RAMOAN and resource scheduling scheme LASA is evaluated. It can be concluded that with the flexibility on traffic aggregation, the cooperative scheme could save substantial energy, and a satisfactory service quality is ensured. These results show that the RAMOAN provides a potential solution for the future access networks.

Appendix 1

The computational method for calculating the probability of an intact ONU-OLT connection is as follows. Here, A_j denote the availability of equipment j.

Since ONU transceiver is wavelength tunable, it can communicate with all four OLT transceivers in an OLT. The probability of an intact connection between an arbitrary ONU and OLT for conventional TWDM scheme is calculated by

$$p_{TWDM} = (1-(1-A_{OLT\_transceiver}A_{OLT\_subsystem})^4)A_{MUX}A_{booster}A_{feeder\_fiber}A_{OA}A_{splitter_{1:4}} A_{node\_distribution\_fiber}A_{splitter_{1:32}}A_{ONU\_distribution\_fiber}A_{ONU\_transceiver}A_{ONU\_subsystem}. \quad (3)$$

While for fully protected TWDM scheme, the probability of an intact ONU-OLT connection is given by

$$\begin{aligned} p_{TWDM-protected} = {} & (1-(1-A_{OLT\_transceiver}A_{OLT\_subsystem})^2)(1-(1-A_{OS_{2:2}})^4)(1-(1-A_{MUX}A_{booster}A_{splitter_{2:1}}A_{feeder\_fiber})^2)A_{OS_{2:2}} \\ & (1-(1-A_{80:20coupler}A_{OA}A_{splitter_{1:4}}A_{node\_distribution\_fiber})(1-A_{OA}A_{splitter_{1:4}}A_{node\_distribution\_fiber}))A_{OS_{2:2}} \\ & (1-(1-A_{80:20coupler}A_{splitter_{1:32}}A_{ONU\_distribution\_fiber})(1-A_{splitter_{1:32}}A_{ONU\_distribution\_fiber}))A_{OS\_2:2} \\ & (1-(1-A_{ONU\_transceiver}A_{ONU\_subsystem})^2). \end{aligned} \quad (4)$$

The probability of an intact ONU-OLT connection for RAMOAN is given by

$$\begin{aligned} p_{RAMOAN} = {} & A_{splitter_{2:1}}(1-(1-A_{MUX}A_{booster}(1-(1-A_{OLT\_transceiver}A_{OLT\_subsystem})^4)) \\ & (1-A_{splitter_{2:4}}A_{MUX}A_{booster}(1-(1-A_{OLT\_transceiver}A_{OLT\_subsystem})^4))) \\ & A_{splitter_{2:4}}A_{coupler_{1:3}}A_{OA}A_{OS_{3:2}}(1-(1-A_{80:20coupler}A_{feeder\_fiber}) \\ & (1-(A_{OS_{2:1}}A_{RN-FL\_interconnection\_fiber}A_{OS_{2:1}}A_{coupler_{1:3}}A_{OA}A_{OS_{3:2}}A_{80:20coupler}A_{feeder\_fiber})^2)) \\ & A_{splitter_{2:32}}A_{OS_{3:2}}(1-(1-A_{80:20coupler}A_{node\_distribution\_fiber}) \\ & (1-(A_{OS_{2:1}}A_{RN-SL\_interconnection\_fiber}A_{OS_{2:1}}A_{coupler_{1:3}}A_{OA}A_{OS_{3:2}}A_{80:20coupler}A_{node\_distribution\_fiber})^2)) \\ & A_{OS_{3:2}}(1-(1-A_{ONU\_transceiver}A_{ONU\_subsystem})^2)(1-(1-A_{ONU\_distribution\_fiber}) \\ & (1-A_{ONU\_interconnection\_fiber}(A_{ONU\_transceiver}A_{ONU\_subsystem})^2A_{OS_{3:2}}A_{ONU\_distribution\_fiber})^2). \end{aligned} \quad (5)$$

Appendix 2

The computational method for calculating the minimal access reach is as follows.
For conventional TWDM scheme, the minimal access reach is given by

$$Reach_{TWDM} = (Power_{launch} + Gain_{booster} - IL_{MUX} + Gain_{OA} - IL_{splitter_{1:4}} - IL_{splitter_{1:32}} - Sensitivity_{receiver}) / IL_{fiber}, \quad (6)$$

while for fully protected TWDM scheme, its minimal access reach is

$$\begin{aligned} Reach_{TWDM-protected} = (&Power_{launch} + Gain_{booster} - IL_{OS_{2:2}} - IL_{MUX} - IL_{splitter_{2:1}} \\ &- IL_{OS_{2:2}} - IL_{80:20coupler} + Gain_{OA} - IL_{splitter_{1:4}} - IL_{OS_{2:2}} - IL_{80:20coupler} \\ &- IL_{splitter_{1:32}} - IL_{OS_{2:2}} - Sensitivity_{receiver}) / IL_{fiber}. \end{aligned} \quad (7)$$

The minimal access reach of RAMOAN depends on its load condition. If the normalized traffic load is below 0.5, the minimal access reach is

$$\begin{aligned} Reach_{RAMOAN} = (&Power_{launch} + Gain_{booster} - IL_{splitter_{2:1}} - IL_{MUX} - IL_{80:20coupler} - IL_{OS_{3:2}} + Gain_{OA} \\ &- IL_{coupler_{1:3}} - IL_{OS_{2:1}} - IL_{RN-FL\_interconnection\_fiber} - IL_{OS_{2:1}} - IL_{OS_{3:2}} - IL_{splitter_{2:4}} \\ &- IL_{80:20coupler} - IL_{OS_{3:2}} - IL_{splitter_{2:32}} - IL_{OS_{3:2}} - Sensitivity_{receiver}) / IL_{fiber}. \end{aligned} \quad (8)$$

When traffic load is between 0.5 and 2/3, the minimal access reach is

$$\begin{aligned} Reach_{RAMOAN} = (&Power_{launch} + Gain_{booster} - IL_{splitter_{2:1}} - IL_{MUX} - IL_{80:20coupler} - IL_{OS_{3:2}} \\ &+ Gain_{OA} - IL_{coupler_{1:3}} - IL_{splitter_{2:4}} - IL_{80:20coupler} - IL_{OS_{3:2}} - IL_{coupler_{1:3}} \\ &- IL_{splitter_{2:32}} - IL_{OS_{3:2}} - Sensitivity_{receiver}) / IL_{fiber}. \end{aligned} \quad (9)$$

When traffic load is beyond 2/3, the minimal access reach is

$$\begin{aligned} Reach_{RAMOAN} = (&Power_{launch} + Gain_{booster} - IL_{splitter_{2:1}} - IL_{MUX} - IL_{80:20coupler} - IL_{OS_{3:2}} \\ &+ Gain_{OA} - IL_{coupler_{1:3}} - IL_{splitter_{2:4}} - IL_{80:20coupler} - IL_{OS_{3:2}} - IL_{splitter_{2:32}} \\ &- IL_{OS_{3:2}} - Sensitivity_{receiver}) / IL_{fiber}. \end{aligned} \quad (10)$$

References

[1] J. Kani, "Power saving techniques for optical access," presented at the *National Fiber Opt. Eng. Conf.*, Los Angeles, CA, USA, Mar. 2012, Paper NM2K.1.

[2] C. Lange and A. Gladisch, "On the energy consumption of FTTH access networks," presented at the *Opt. Fiber Commun. Conf. Expo.*, San Diego, CA, USA, Mar. 2009, Paper JThA79.

[3] Y. Lv, N. Jiang, K. Qiu, and C. Xue, "Study on the energy-efficient scheme based on the interconnection of optical-network-units for next generation optical access network," *Opt. Commun.*, vol. 332, pp. 114–118, Dec. 2014.

[4] N. Jiang, D. Liu, Y. Lv, and K. Qiu, "An efficient energy-saving scheme based on grouping of ONU for optical access network," *IEEE Photon. J.*, vol. 7, no. 2, Apr. 2015, Art. no. 791207.

[5] J. Li, H. He, M. Bi, Y. Tian, and W. Hu, "Energy-efficient selective sampling receiver for OFDMA-PON," in *Proc. Int. Conf. Asia Commun. Photon.*, Beijing, China, Nov. 2013, Paper AF1G.3.

[6] B. Wang, P. Ho, and C. Lin, "A novel energy-efficient transmission scheme in CO-OFDM elastic optical networks," *J. Lightw. Technol.*, vol. 32, no. 21, pp. 3380–3388, Nov. 2014.

[7] M. Bolea, R. P. Giddings, M. Bouich, C. Aupetit-Berthelemot, and J. M. Tang, "Digital filter multiple access PONs with DSP-enabled software reconfigurability," *J. Opt. Commun. Netw.*, vol. 7, no. 4, pp. 215–222, Apr. 2015.

[8] X. Duan, R. P. Giddings, S. Mansoor, and J. M. Tang, "Experimental demonstration of upstream transmission in digital filter multiple access PONs with real-time reconfigurable optical network units," *J. Opt. Commun. Netw.*, vol. 9, no. 1, pp. 45–52, Jan. 2017.

[9] C. Lange *et al.*, "Energy efficiency of load-adaptively operated telecommunication networks," *J. Lightw. Technol.*, vol. 32, no. 4, pp. 571–590, Feb. 2014.

[10] M. P. I. Dias, D. P. Van, L. Valcarenghi, and E. Wong, "Energy-efficient framework for time and wavelength division multiplexed passive optical networks," *J. Opt. Commun. Netw.*, vol. 7, no. 6, pp. 496–504, Jun. 2015.

[11] L. Wang *et al.*, "Dynamic bandwidth and wavelength allocation scheme for next-generation wavelength-agile EPON," *J. Opt. Commun. Netw.*, vol. 9, no. 3, pp. B33–B42, Mar. 2017.

[12] A. Dixit, B. Lannoo, D. Colle, M. Pickavet, and P. Demeester, "ONU power saving modes in next generation optical access networks: Progress, efficiency and challenges," *Opt. Exp.*, vol. 20, no. 26, pp. B52–B63, Dec. 2012.
[13] A. Dixit, B. Lannoo, D. Colle, M. Pickavet, and P. Demeester, "Energy efficient dynamic bandwidth allocation for Ethernet passive optical networks: Overview, challenges, and solutions," *Opt. Switch. Netw.*, vol. 18, pp. 169–179, Nov. 2015.
[14] M. P. I. Dias and E. Wong, "Performance evaluation of VCSEL ONU using energy-efficient just-in-time dynamic bandwidth allocation algorithm," in *Proc. Int. Conf. Photon. Global*, Singapore, Dec. 2012, Paper 1-5.
[15] M. P. I. Dias and E. Wong, "Sleep/doze controlled dynamic bandwidth allocation algorithms for energy-efficient passive optical networks," *Opt. Exp.*, vol. 21, no. 8, pp. 9931–9946, Apr. 2013.
[16] D. P. Van, L. Valcarenghi, M. P. I. Dias, K. Kondepu, P. Castoldi, and E. Wong, "Energy-saving framework for passive optical networks with ONU sleep/doze mode," *Opt. Exp.*, vol. 23, no. 3, pp. A1–A14, Feb. 2015.
[17] Y. Lv, N. Jiang, K. Qiu, and C. Xue, "Energy-efficient load adaptive polling sequence arrangement scheme for passive optical access networks," *J. Opt. Commun. Netw.*, vol. 7, no. 6, pp. 516–524, Jun. 2015.
[18] International Telecommunication Union, Passive optical network protection considerations, ITU-T G.Sup 51, 2016.
[19] J. Song *et al.*, "Energy efficiency evaluation of tree-topology 10 gigabit Ethernet passive optical network and ring-topology time- and wavelength-division-multiplexed passive optical network," *Opt. Eng.*, vol. 54, no. 9, Sep. 2015, Art. no. 090502.
[20] Y. Lv, N. Jiang, C. Xue, and K. Qiu, "An energy-efficient and robust ring network structure for next generation optical access," in *Proc. Int. Conf. Lasers Electro-Opt.*, San Jose, CA, USA, Jun. 2016, Paper JTh2A.17.
[21] E. Wong, "Survivable architectures for time and wavelength division multiplexed passive optical networks," *Opt. Commun.*, vol. 325, pp. 152–159, Apr. 2014.
[22] OASE project, D4.2.1: Technical assessment and comparison of next generation optical access system concepts, Oct. 2011.
[23] A. Dixit, B. Lannoo, G. Das, D. Colle, M. Pickavet, and P. Demeester, "Flexible TDMA/WDMA passive optical network: Energy efficient next-generation optical access solution," *Opt. Switch. Netw.*, vol. 10, pp. 491–506, Apr. 2013.
[24] K. Grobe, M. Roppelt, A. Autenrieth, J. Elbers, and M. Eiselt, "Cost and energy consumption analysis of advanced WDM-PONs," *IEEE Commun. Mag.*, vol. 49, no. 2, pp. S25–S32, Feb. 2011.
[25] [Online]. Available: http://www.china-tscom.com/en/product/plist.aspx?menuid = 0203020403
[26] [Online]. Available: http://www.lightwavelink.com.tw/products/en.shtml
[27] G. Kramer, B. Mukherjee, S. Dixit, Y. Ye, and R. Hirth, "Supporting differentiated classes of service in Ethernet passive optical networks," *J. Opt. Netw.*, vol. 1, no. 8, pp. 280–298, Aug./Sep. 2002.